Calculation of Apparent pK_a Values of Saturated Fatty Acids With Different Lengths in DOPC Phospholipid Bilayers

Sanja Škulj, Mario Vazdar*

Division of Organic Chemistry and Biochemistry, Rudjer Bošković Institute, Bijenička 54, HR-10000 Zagreb, Croatia

*Corresponding author: e-mail : mario.vazdar@irb.hr

Abstract

We performed all-atom molecular dynamics simulations and calculated free energy profiles and pK_a values for neutral and anionic forms of single myristic (C14:0), palmitic (C16:0) and stearic (C18:0) fatty acid in the DOPC bilayer and explicit solvent. We showed that neutral forms of fatty acids are stabilized inside the bilayer by hydrogen bonding of fatty acid carboxylic group with DOPC phosphate and carbonyl group. In contrast to the neutral form, anionic fatty acids are shifted towards water-membrane interface and are instead stabilized by hydrogen bonding to interfacial water. By using umbrella sampling simulations, we calculated free energies of stabilization and revealed that free energy of stabilization inside the bilayer increases with the chain length for both neutral and deprotonated forms. On the other hand, free energies of flip-flop of neutral forms are constant upon the prolongation of the fatty acid. Based on the free energy curves, we also calculated apparent fatty acid p$K_{a,app}$ values in the bilayer which are 6.70, 6.94 and 6.63 for myristic, palmitic and stearic acid. By further analysis of the calculated curves we found that spontaneous protonation of fatty acid anions takes place in the bilayer interior at ca. 1.5 nm from the bilayer center for all studied fatty acids.

Introduction

An adequate intake of free long-chain fatty acids (FFA) is essential for cells and organism growth and development.[1,2] FFAs can easily flip-flop across the bilayer in their neutral form according to the concentration gradient and without the need for protein assistance.[3–7] On the other hand, the transport of the anionic form is far more difficult and has not been experimentally detected since the energy penalty for bringing the charged molecule across the bilayer is very high and is probably assisted by the cellular membrane protein machinery, in particular uncoupling proteins (UCPs).[5,8–10] Interestingly, the transport of protons across bilayers with incorporated UCPs assisted by fatty acids also depends on the length of the saturated fatty acid chain and decreases with the chain length if it is longer than 12 carbon atoms.[11] This is in contrast to the well-known Overton rule[12] which predicts that upon the increase of the hydrophobicity, diffusion across bilayers should increase. This discrepancy has been attributed to the lower solubility of longer fatty acids in water in comparison to the shorter ones and not to actual decreased membrane permeability of longer fatty acids.[6] Importantly, it has been found that proton transport across the bilayer increases with the degree of unsaturation of fatty acid,[10] further implying the importance of fatty acid in the proton transport.

In addition to adsorption and desorption of fatty acids at/from the bilayer, the flip-flop of fatty acids across membranes constitutes a key step in the proton transport mechanism. Since only neutral fatty acids can effectively cross the bilayer, the equilibrium ratio of neutral/anionic forms of fatty acids, i. e. the apparent pK_a value of fatty acids in the bilayer, is essential for better understanding of the process. Due to different hydration and water dynamics in the bilayer interior where fatty acids are incorporated,[13,14] the protonation state of the fatty acid differs significantly from the bulk phase which results in the shift of apparent pK_a of the fatty acid in the bilayer towards higher values in the hydrophobic environment[15] as compared to the bulk where its estimated value is around 4.75. Experimental determination of fatty acid pK_a values is difficult and gives values which significantly differ from each other depending on the used experimental technique.[16–20] In our recent work, we have determined experimental pK_a values of FFAs by measuring zeta-potential of liposomes reconstituted with 40 mol% of FFAs. Notably, pK_a values increase with chain length for saturated FFAs (in the range of 6.25 – 7.28 for C16:0 – C20:0) and

decrease with the number of double bonds (in the range of 7.28 – 6.13 for C20:0 – C20:4). This effect has been explained by analyzing the differences in the hydrophobic interactions between lipid acyl chains and incorporated FFAs which depend on the FFA chain length.[21]

So far, to the best of our knowledge, there are several papers dealing with pK_a calculations using constant pH molecular dynamics and/or coarse grained molecular dynamics,[22–26] but none of them have dealt with the pK_a dependence on the fatty acid length in a systematic manner. Therefore, in this work we use all-atom molecular dynamics (MD) simulations in the combination with free energy umbrella sampling calculations and explicit solvent to theoretically determine the pK_a values of the fatty acids in 1,2-dioleoyl-sn-glycero-3-phosphocholine (DOPC) bilayers depending on the fatty acids length.

Computational details

In order to understand the details of the H$^+$ transport via fatty acid flip-flop, we considered neutral and anionic form of three long-chain free fatty acids: myristic acid (C14:0), palmitic (C16:0) and stearic (C18:0) acid in the 1,2-dioleoyl-*sn*-glycero-3-phosphocholine bilayer. To provide a reasonable model for a DOPC membrane, we constructed the system which contained 64 lipids per leaflet, ca. 11500 water molecules, a single fatty acid and Na$^+$ ion in the anionic form of FFA for neutralization. Molecular dynamics simulations were performed in a periodic box with the size of ca. 6.5 nm x 6.5 nm x 12.3 nm. Slipids force field[27–29] was used for DOPC molecules and fatty acids and TIP3P[30] for water. Atomic charges for all neutral and anionic forms of FFAs were calculated by the protocol used for Slipids force field parameterization[27], i.e. Merz-Singh-Kollman scheme[31] with the B3LYP/6-31G(d) optimized geometry followed by a single point ESP charge calculation using B3LYP/cc-pVTZ level of theory. RESP method[32] was used to obtain the final charge refinement of the FFA by using AMBER Antechamber module.[33] All simulations were performed at constant temperature of 310 K employing the Nosé–Hoover thermostat[34] independently for the DOPC bilayer/FFA and water subsystems with a coupling constant of 0.5 ps^{-1}. Pressure was held at 1 bar using the semi-isotropic Parrinello-Rahman barostat[35] with the time constant for pressure coupling of 10 ps^{-1}. Electrostatics were obtained by the particle-mesh

Ewald (PME) method[36] with the real space Coulomb interactions cut off at 1 nm using a Fourier spacing of 0.12 nm with the Verlet cut-off scheme. All FFAs were placed in the DOPC bilayer and simulated for 200 ns of classical molecular dynamics. Initial configurations for umbrella sampling simulations were generated from two independent simulations, where a single FFA molecule (neutral and anionic form) was pulled from the equilibrium position in each of the leaflets towards water phase and bilayer center, respectively, using force of 1000 kJ mol^{-1} nm^{-2} and rate of 0.001 nm ps^{-1}. In this way, we obtained 90 initial configurations for each system spanning distances from -4.5 to 4.5 nm from the bilayer center in z direction thus covering the whole bilayer. In order to properly sample translocation of FFA anion across the bilayer center and to remove artefacts resulting from too strong interaction of FFA anion and lipid phosphate groups, we performed replica exchange umbrella sampling simulations (REUS) for the anionic form of all FFAs in the range of -2 nm to 2 nm (in total 40 configurations per FFA), similar to previously published procedures.[37,38] Exchanges between adjacent replicas were attempted every 2 picoseconds between neighboring replica pairs. A harmonic restraint with a force constant of 1000 kJ mol^{-1} nm^{-2} was applied to the distance between the carbon atom of carbonyl group in fatty acid and the centre of mass of the bilayer with 0.1 nm spacing between biasing potentials. In REUS simulations, force constants of 2000 and 3000 kJ mol^{-1} nm^{-2} were used for four configurations around the bilayer center, with spacing of 0.07 nm between them. For each fatty acid the simulation time of 30 ns per umbrella window was used with a 2 fs time step, except for REUS simulations where simulation time was 40 ns per umbrella window. First 5 ns were considered as equilibration in each window and were discarded from the further analysis. Potential of mean force (PMF) calculations were performed using the umbrella sampling, while the weighted histogram analysis method (WHAM) was used to calculate the PMFs from the biased distributions.[39] Final free energy curves were obtained by symmetrization of the profiles in each of the leaflets and error bar were calculated using the Bayesian bootstrap analysis with 50 bootstraps.[39] Free energy profiles were set to zero in bulk water for all anionic forms, and all neutral forms were shifted by free energy of protonation in water of 3.2 kcal mol^{-1} assuming pK_a value of all fatty acids in water is 4.75[40] and pH of water solution is 7. We calculated pK_a values in

membranes as a function of z from the PMFs difference between shifted anionic and neutral form $\Delta\Delta G_a$ according to the following expressions:[41,42]

$$\Delta pK_a = \frac{\Delta\Delta G_a}{2.303RT} \qquad (1)$$

$$pK_a = pH + \Delta pK_a \qquad (2)$$

Finally, the apparent $pK_{a,app}$ value of fatty acids was calculated using equilibrium free energies of anionic and neutral fatty acid (shifted by free energy of deprotonation of 3.2 kcal mol^{-1}). All simulations were run with the GROMACS 5.1.4 software package[43] with PLUMED 2.4 plugin[44] while quantum chemical calculations were performed using Gaussian 09.[45]

Results and discussion

In this section, we present density profiles, hydrogen bonding capabilities and free energy profiles of free fatty acids, separately for neutral and anionic form in the DOPC bilayer. Both forms exist in yet undetermined ratio in the bilayer, depending on their pK_a value which is different than pK_a values in water due to hydrophobic environment of the bilayer,[15] and are equally important for theoretical determination of their acidity using equations (1) and (2). Figure 1 shows number density profiles for myristic (C14:0), palmitic (C16:0) and stearic acid (C18:0) in neutral and anionic forms, respectively, immersed in DOPC bilayer after 200 ns of simulation. In the case of neutral FFAs, the fatty acid carboxylic group is inserted deeper in the bilayer, below the DOPC carbonyl group (Figures 1a-c). In contrast, the carboxylic group of the anionic form is by ca. 0.5 nm shifted towards water-membrane interface, and located between the DOPC phosphate and DOPC carbonyl group (Figure 1, d-e). Interestingly, this position shift is almost constant for all fatty acids regardless of the fatty acid chain length as previously shown in MD simulations with high concentrations of FFAs in DOPC bilayer.[21] We also see that almost all other elements of density profiles for both neutral and anionic fatty acids look very similar on a first sight, and equilibrium positions of selected groups is changed slightly upon prolongation of the fatty acid chain. The small differences are visible in the position of the fatty acid center of mass and terminal carbon

atoms which gently move towards the bilayer interior, both for neutral and anionic fatty acids. Notably, the number density maximum for terminal carbon atom is shifted across the bilayer center for neutral C16:0 and especially for neutral C18:0 FFA (Figure 1, b-c). The deeper location of neutral fatty acids compared to anionic forms, together with the increase of the insertion depth, have also been observed experimentally for fluorescent probes attached to fatty acids by using parallax analysis of fluorescence quenching.[46]
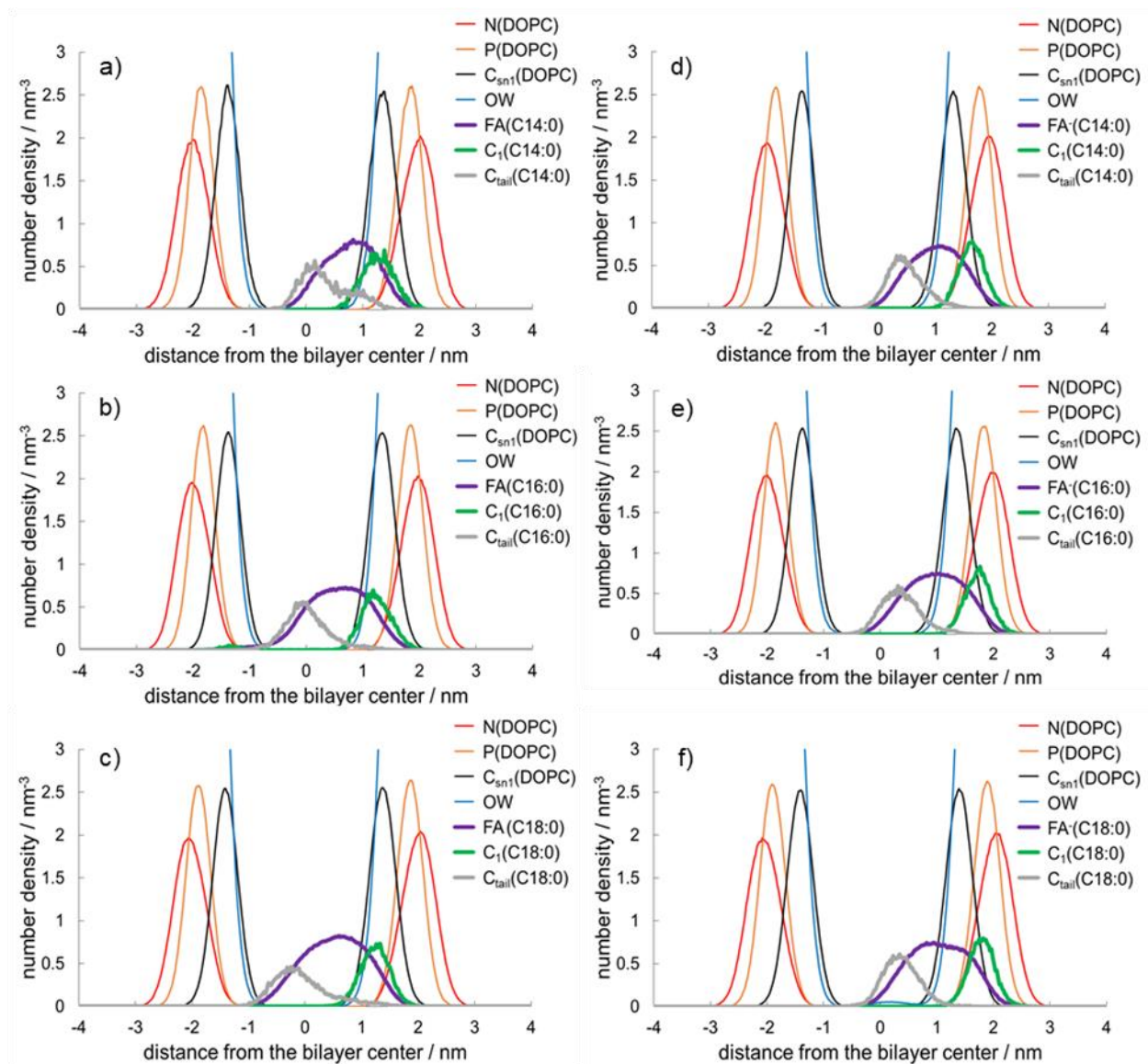

Figure 1. Number density profiles of neutral myristic, palmitic and stearic acid (a-c) and anionic myristic, palmitic and stearic acid (d-f). Number density of DOPC nitrogen atom is shown in red, DOPC phosphate atom is shown in orange, DOPC sn1 carbonyl atom is shown in black and oxygen water atom is shown in blue color. Number density of neutral

(a-c) and anionic fatty acid (d-f) center of mass are shown in purple, number density of carboxylic carbon atom C_1 of neutral (a-c) and anionic fatty acid (d-f) is shown in green (magnified by a factor of 20), whereas number density of terminal carbon atom C_{tail} is shown in light grey color (magnified by a factor of 20).

The physical reason behind different equilibrium position of neutral/anionic forms is in the ability of neutral carboxylic group to make hydrogen bonds with the DOPC phosphate and carbonyl groups, in contrast to anionic form of the acid. This is visualized in Figures 2 and 3, where radial distribution functions (RDFs) between P atom of DOPC phosphate group (Figure 2) and C atom of DOPC carbonyl group belonging to sn1 chain and vs. C atom of carboxylic acid group (Figure 3), respectively, are presented. We chose the phosphorus and carbon atoms of DOPC and fatty acids in order to simplify analysis of hydrogen bonding capability. Analysis of the results show that the first RDF maximum between neutral fatty acid carboxylic group vs. both DOPC phosphate (Figure 2a) and DOPC carbonyl group (Figure 3a) is shifted toward smaller interatomic distances of ca. 0.45 nm and followed by the less pronounced second RDF maximum at around 0.85 nm for both groups. Moreover, the first and second maxima are located at the same distance corresponding to hydrogen bonding between neutral fatty acid carboxylic group serving as hydrogen bond donors and DOPC phosphate and carbonyl groups which act as hydrogen bond acceptors. In particular, hydrogen bonding is stronger towards DOPC carbonyl group, which is evidenced by more pronounced maximum in the RDF compared to DOPC phosphate group (Fig. 2, a). It is also interesting to note that there are no large differences in the RDFs between fatty acids themselves, i. e. there are no substantial quantitative differences in hydrogen bonding capability regardless of the fatty acid chain length. Conversely, in the case of anionic fatty acids, the first RDF maximum between carboxylic group and DOPC phosphate group is shifted towards larger interatomic distances of ca. 0.60 nm, followed by the second RDF maximum at around 0.80 nm (Figure 2, b) which indicates no formation of hydrogen bond since the corresponding atoms are too far away, instead forming a solvent separated pair. In the case of RDFs between carboxylic group and DOPC carbonyl group, the first maxima are located at ca 0.55 nm whereas the second maximum in the RDF are not pronounced (Figure 3, b).
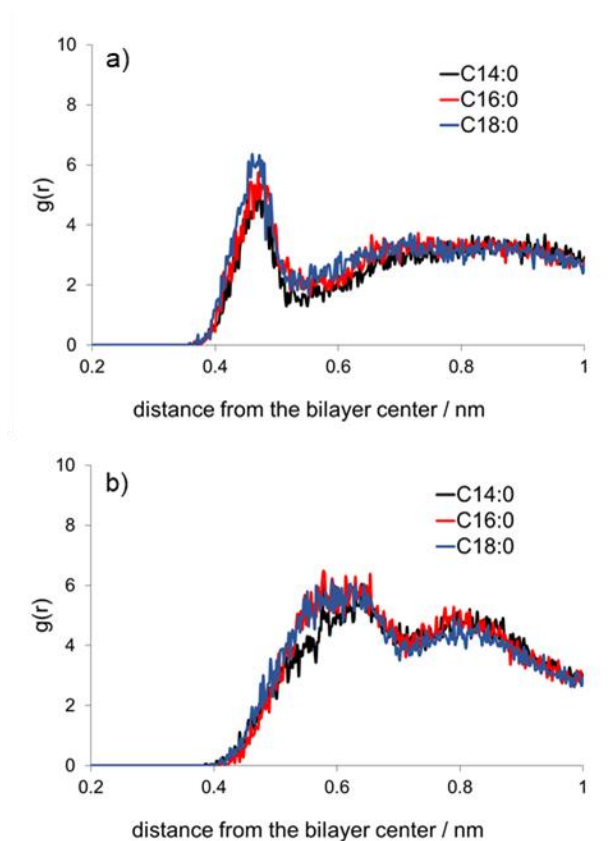
Figure 2. Radial distribution functions g(r) between carboxylic carbon atom of neutral fatty acid and DOPC phosphorus atom (a) and between carboxylic carbon atom of anionic fatty acid and DOPC phosphorus atom (b) for myristic (black), palmitic (red) and stearic fatty acid (blue).
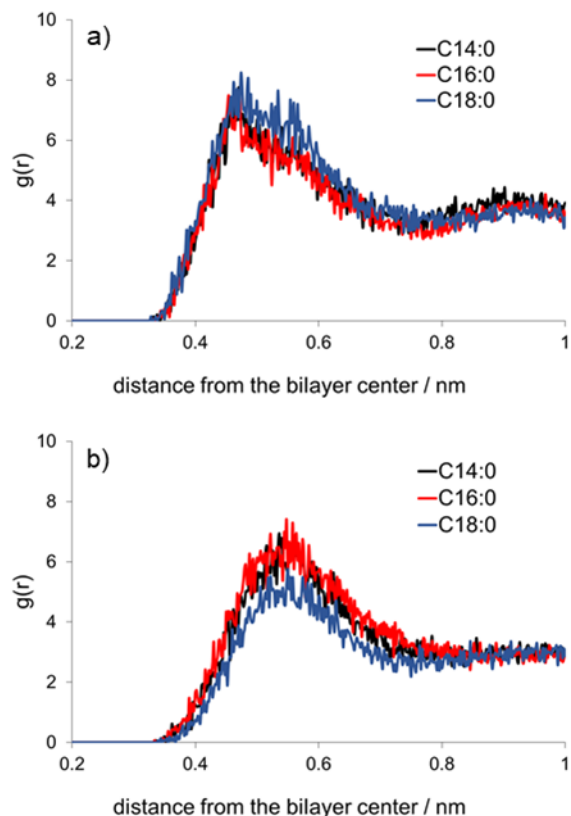
Figure 3. Radial distribution functions g(r) between carboxylic carbon atom of neutral fatty acid and DOPC carbonyl sn1 atom (a) and between carboxylic carbon atom of anionic fatty acid and DOPC carbonyl sn1 atom for myristic (black), palmitic (red) and stearic fatty acid (blue).

Now we turn to the analysis of free energy profiles for neutral and anionic forms of fatty acids in the bilayer. Figure 4a shows free energy profiles of neutral and anionic fatty acids in the DOPC bilayer. We see that neutral fatty acids are getting more stabilized with the chain length as evidenced in free energy of stabilization $\Delta\Delta G_{stabilization}$, being -9.8 ± 0.2 kcal mol^{-1} for myristic acid, -11.3 ± 0.2 kcal mol^{-1} for palmitic acid and -13.0 ± 0.1 kcal mol^{-1} for stearic acid (Table 1). As free energy profiles show, the neutral form of fatty acids is stabilized inside the bilayer, with the minimum located at ca. 1.0 – 1.2 nm from the bilayer center. There is a small shift in the equilibrium position between fatty acids, but it is very difficult to quantify it due to the shallow energy minimum. Upon translocation of the fatty acid across the bilayer, there is no pronounced maximum in the bilayer center, and an energy plateau is formed instead indicating that the

neutral form of fatty acid is more stable in the center of the bilayer than in the water phase. Free energy barriers for the flip-flop of neutral fatty acid $\Delta\Delta G_{flip\text{-}flop}$ are 3.0 ± 0.3 kcal mol^{-1} for myristic acid, 3.0 ± 0.3 kcal mol^{-1} for palmitic acid and 3.1 ± 0.2 kcal mol^{-1} for stearic acid (Figure 4a), similar to recent replica exchange umbrella sampling simulations for transfer of neutral palmitic acid across prototypical yeast membranes[38] and other computational studies[3,26]. The calculated low flip-flop barrier heights would imply the very fast flip-flop of neutral fatty acids across bilayers that is in agreement with previous experimental work by Hamilton group.[4,47,48] Moreover, these values also go along with experimental conductance measurements of proton transport by Gutknecht[49] who has shown that the proton conductance across bilayers induced by fatty acids is independent on the chain length as suggested by the present MD simulations.
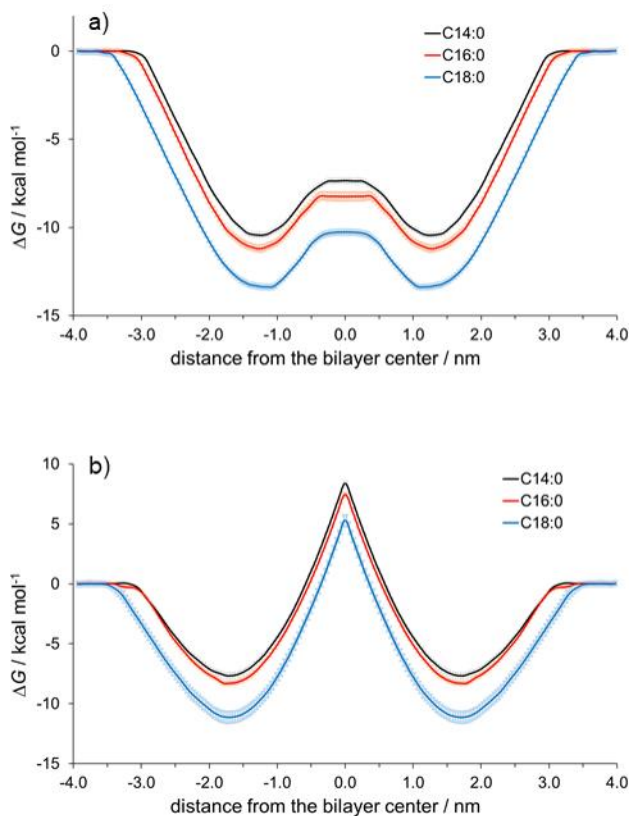

Figure 4. Free energy profiles for neutral myristic (black), palmitic (red) and stearic acid (blue) are shown in panel a). Free energy profiles for anionic myristic (black), palmitic (red) and stearic acid (blue) are shown in panel b). Free energy profiles are symmetrized between the leaflets.

Table 1. Free energies of stabilization $\Delta\Delta G_{stabilization}$ of different fatty acids for neutral and anionic form of fatty acid (in kcal mol^{-1}) together with the apparent pK_a values p$K_{a,app}$.

fatty acid	C14:0		C16:0		C18:0	
	neutral	*anion*	*neutral*	*anion*	*neutral*	*anion*
$\Delta\Delta G_{stabilization}$	-9.8 ± 0.2	-7.8 ± 0.3	-11.3 ± 0.2	-8.3 ± 0.2	-13.0 ± 0.1	-11.2 ± 0.5
$\Delta\Delta G_{flip\text{-}flop}$	3.1 ± 0.3	16.0 ± 0.4	3.0 ± 0.3	15.7 ± 0.2	3.1 ± 0.2	16.4 ± 0.7
p$K_{a,app}$	6.70 ± 0.10		6.94 ± 0.08		6.63 ± 0.14	

On the other hand, behavior of anionic form of fatty acid in the bilayer is quantitatively different. In particular, anionic forms are as less stabilized in the bilayer headgroup region, as compared to neutral FFAs, with free energies of stabilization $\Delta\Delta G_{stabilization}$ of -7.8 ± 0.3 kcal mol^{-1}, -8.3 ± 0.2 kcal mol^{-1} and -11.2 ± 0.5 kcal mol^{-1} kcal mol^{-1} for myristic, palmitic and stearic acid anion (Table 1) which show minima at ca. 1.6 – 1.8 nm from the bilayer center close to the water interface (Figure 4b). Upon translocation across the bilayer, the anionic form of the acid has to cross a significant free energy barrier $\Delta\Delta G_{flip\text{-}flop}$ of 16.0 ± 0.4 kcal mol^{-1}, 15.7 ± 0.2 kcal mol^{-1} and 16.4 ± 0.7 kcal mol^{-1} for myristic, palmitic and stearic acid, respectively (Table 1). These high barriers are connected to the transfer of a charged group through strongly hydrophobic bilayer interior and are close to the values obtained also for different ions, such as K$^+$, Na$^+$, Cl$^-$,[50,51] charged amino acids,[42] and are also similar to other simulation studies of fatty acid anions.[26,38] Interestingly, the free energy barriers for anion translocation are independent on the chain length, similar to neutral fatty acids.

In the next step, we used free energy curves of neutral and anionic fatty acid forms to calculate pK_a values in membranes using equations (1) and (2) as shown in Figure 5. The pK_a value of carboxylic group in water is 4.75 and it is used as a reference for all simulated FFAs due to their hydrophobicity and insolubility and in turn inability to determine the pK_a values in water.[52] In order to determine the apparent p$K_{a,app}$ value of the fatty acid in the bilayer, we used the equations (1) and (2), and obtained following p$K_{a,app}$ values of 6.70 ± 0.10, 6.94 ± 0.08 and 6.63 ± 0.14 for myristic, palmitic and stearic acid in the DOPC bilayer, showing no significant difference of p$K_{a,app}$ values with the chain length.

Figures S1 – S6 show convergence of free energies as a function of simulation time for symmetrized profiles. We see that 25 ns of sampling is sufficient to converge the free energy for

both neutral and anionic FFA up to less than 0.6 kcal mol^{-1}, as well as pK_a values (Table S1). Nevertheless, the final converged free energy values of stabilization on each side slightly differ (up to 1.6 kcal mol^{-1}) which is a consequence of insufficient sampling insertion/desorption events of the fatty acid at the membrane interface which can be resolved only at very long time scales and large bilayer setups.[53]

The calculated results which show no increase of pK_a values with the chain length are in agreement with experimental NMR values for palmitic and stearic acid where no substantial difference in measured pK_a values for 3.3 mol% of myristic, palmitic and stearic acid in PC vesicles have been observed, being in the range of 7.2 – 7.4.[16,17] Also, these results are at odds with the observed increase of experimentally determined p$K_{a,app}$ values with chain length obtained by zeta-potential measurements for DOPC liposomes with 40 mol% of incorporated FFAs.[21] We should mention here that a direct comparison between theoretical estimation of p$K_{a,app}$ values in infinitely diluted systems such as ours and those obtained by different experimental techniques with finite concentration of FFAs is not possible, since the apparent experimental pK_a values depend on the concentration of fatty acids in the bilayer and their mutual interaction, but also on salt concentration, temperature and other factors.[54] This is especially visible when pK_a values of monolayers consisted of fatty acids are examined, where pK_a values increase with the fatty acid chain length assuming values in the range of 6 – 9 for chain lengths of $C_8 – C_{16}$, and are significantly higher as compared to the corresponding pK_a values in membranes.[18] This poses an interesting question for future investigations of systems with finite concentrations of FFAs in membranes, since it is known that the concentration of FFAs in cellular membranes varies depending on many physiological factors[55] and high concentration of FFA is essential for cancer cell proliferation.[56]

Since the pK_a of FFAs is smaller than the pH of aqueous phase which is assumed to be strictly neutral with the value of 7, the fatty acids exist dominantly as anionic species in water phase. Therefore, the neutral form of the acid is less stable in water and it takes 3.2 kcal mol^{-1} to protonate it (see Computational Details). However, upon the translocation of the anionic form across the bilayer at the distance of ca. 1.5 nm from the bilayer center, the free energies of the neutral and the anionic form become equal (Figure 5). After this threshold distance, the neutral

form becomes more stable in the bilayer center instead of energetically unfavorable anionic form, being actually the dominant form transferred across the bilayer.[41,42]

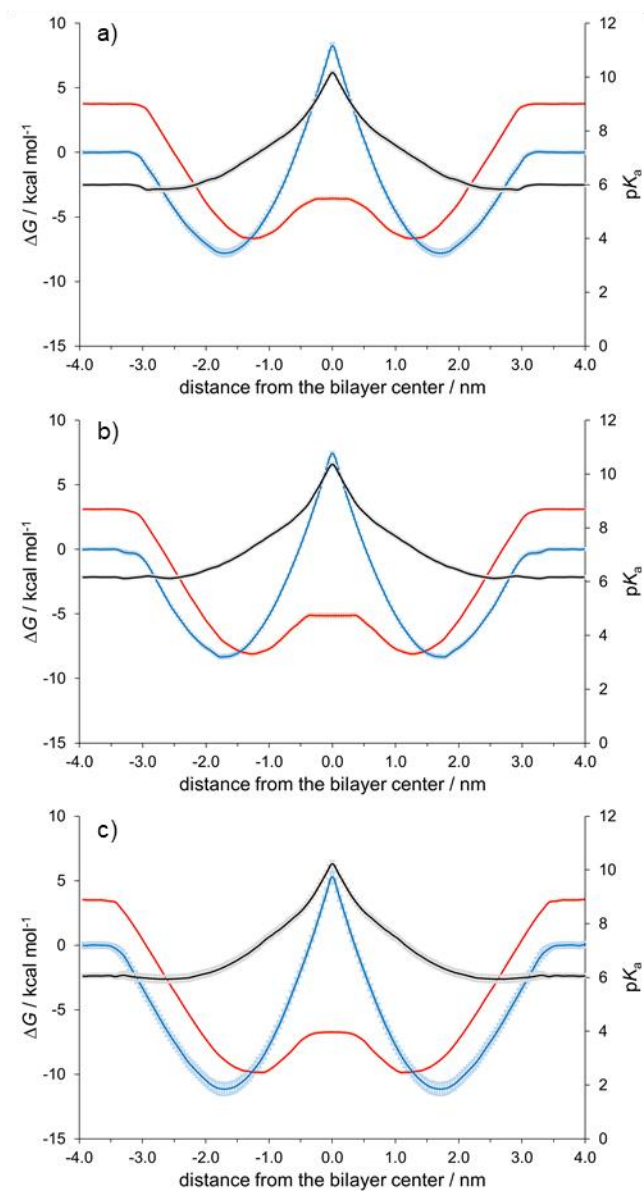

Figure 5. Free energy profiles of stabilization for neutral (red) and anionic fatty acid (blue) with calculated pK_a values (black) for myristic, palmitic, and stearic acid. Free energy and pK_a profiles are symmetrized between the leaflets.

The proximity of two energy minima for neutral and anionic form separated by a small barrier of about 1 – 2 kcal mol^{-1} also implies that a rapid interchange between neutral and anionic form of fatty acid exists in the equilibrium. Due to spontaneous protonation in the hydrophobic environment,[15] we can construct the hybrid free energy profile of translocation by merging free energy profiles for neutral and anionic forms at the position where two curves intersect (Figure 6). In our case, the hybrid lowest free energy barriers for translocation are 4.2 ± 0.4 kcal mol^{-1} and 3.2 ± 0.3 kcal mol^{-1} and 4.4 ± 0.5 kcal mol^{-1}, for myristic, palmitic and stearic acid, respectively (Figure 6).
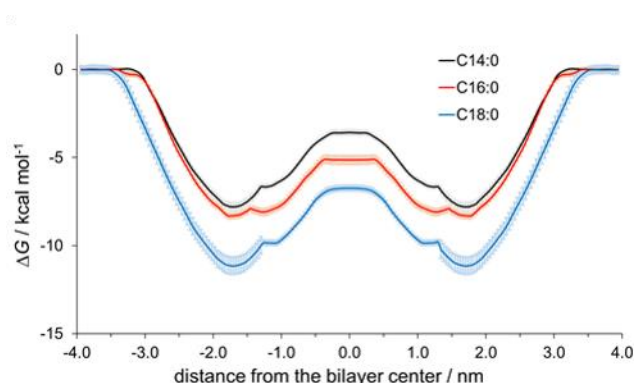

Figure 6. Hybrid free energy profiles for translocation of anionic forms of myristic, palmitic and stearic acid. Free energy profiles are symmetrized between the leaflets.

In this way we obtained only a crude approximation of the lowest free energy curve for translocation of anion, since protonation/deprotonation can also occur at different positions in the bilayer with different probabilities, not only at the intersection point of corresponding free energy curves. Nevertheless, permeabilities of ionic species calculated from hybrid free energy profiles have been shown to be closer to experimental values by several orders of magnitude than those calculated from free energy profiles for ion translocation alone, thus endorsing the existence of spontaneous protonation/deprotonation in the bilayer.[41,57] We also believe that a possibility of spontaneous protonation of fatty acid anions in biological membranes shown in this work can help in elucidating the mechanism of fatty acid transport across the bilayers, offering an additional possibility of anion transfer across membranes in addition to protein-assisted mechanism.[5]

Conclusions

Using molecular dynamics simulations, we showed that the stabilization of the neutral form in the bilayer with respect to water phase increases with the fatty acid chain length, ranging from -9.8 kcal mol^{-1} for myristic acid, -11.3 kcal mol^{-1} for palmitic acid and -13.0 kcal mol^{-1} for stearic acid. Neutral forms of fatty acids are stabilized inside the bilayer due to hydrogen bond formation of carboxylic –OH group with DOPC phosphate and carbonyl groups. The free energy barrier for translocation is independent of the fatty acid chain length and very low, being around ca. 3 kcal mol^{-1} for all studied acids thus confirming an experimental observation that the flip-flop of the FFA neutral forms is very fast[4] in agreement with other computational results.[3,19,24–26] On the other hand, the transport of the anionic form of FFA across the bilayer is qualitatively different. In a first place, there is no hydrogen bonding with of negatively charged carboxylic group with DOPC phosphate and carbonyl groups and fatty acid anion is shifted towards the water membrane interface where it easily makes hydrogen bonds with water at the interface thus being less stabilized by ca. 2 – 3 kcal mol^{-1} as compared to the neutral forms and assuming values of -7.8, -8.3 and -11.2 kcal mol^{-1} for myristate, palmitate and stearate with similar flip-flop energy barriers of ca. 16 kcal mol^{-1}. However, due to spontaneous protonation of FFA anion in the membrane and a very small barrier connecting these minima, the translocation barriers of anions are significantly lowered and comparable to the translocation barriers of neutral fatty acids. Finally, using free energy curves of neutral and anionic forms, we were able to calculate pK_a values for myristic, palmitic and stearic acid which are 6.70, 6.94 and 6.63 being in agreement with available experimental NMR data. The change of protonation state of fatty acid upon translocation of anionic form resulting in significantly lowered hybrid free energy barriers, has important implications in future studies of proton transfer mechanism across more realistic biological membranes with different concentrations of embedded fatty acids.

Supporting Information

Figures S1 - S13 and Table S1 showing convergence of free energy profiles and p$K_{a,app}$ values in different bilayer leaflets. This material is available free of charge via the Internet at http://pubs.acs.org.

References

(1)   Berg, J. M.; Tymoczko, J. L.; Stryer, L. *Biochemistry*; W H Freeman: New York, 2002.

(2)   McArthur, M. J.; Atshaves, B. P.; Frolov, A.; Foxworth, W. D.; Kier, A. B.; Schroeder, F. Cellular Uptake and Intracellular Trafficking of Long Chain Fatty Acids. *J. Lipid Res.* **1999**, *40* (8), 1371–1383.

(3)   Wei, C.; Pohorille, A. Flip-Flop of Oleic Acid in a Phospholipid Membrane: Rate and Mechanism. *J. Phys. Chem. B* **2014**, *118* (45), 12919–12926.

(4)   Kamp, F.; Hamilton, J. a. PH Gradients Across Phospholipid Membranes Caused by Fast Flip-Flop of Un-Ionized Fatty Acids. *Proc. Natl. Acad. Sci. U. S. A.* **1992**, *89* (December), 11367–11370.

(5)   Hamilton, J. A.; Guo, W.; Kamp, F. Mechanism of Cellular Uptake of Long-Chain Fatty Acids: Do We Need Cellular Proteins? *Mol. Cell. Biochem.* **2002**, *239* (1–2), 17–23.

(6)   Kamp, F.; Hamilton, J. A. How Fatty Acids of Different Chain Length Enter and Leave Cells by Free Diffusion. *Prostaglandins Leukot. Essent. Fat. Acids* **2006**, *75* (3), 149–159.

(7)   Pohl, E. E.; Peterson, U.; Sun, J.; Pohl, P. Changes of Intrinsic Membrane Potentials Induced by Flip-Flop of Long- Chain Fatty Acids. *Biochemistry* **2000**, *39* (7), 1834–1839.

(8)   Skulachev, V. P. Fatty Acid Circuit as a Physiological Mechanism of Uncoupling of Oxidative Phosphorylation. *FEBS Lett.* **1991**, *294* (3), 158–162.

(9)   Garlid, K. D.; Orosz, D. E.; Modrianska, M.; Vassanelli, S.; Jezek, P. On the Mechanism of Fatty Acid-Induced Proton Transport by Mitochondrial Uncoupling Protein. *J. Biol. Chem.* **1996**, *271* (5), 2615–2620.

(10)   Beck, V.; Jaburek, M.; Demina, T.; Rupprecht, A.; Porter, R. K.; Jezek, P.; Pohl, E. E. Polyunsaturated Fatty Acids Activate Human Uncoupling Proteins 1 and 2 in Planar Lipid Bilayers. *FASEB J.* **2007**, *21* (4), 1137–1144.

(11)   Winkler, E.; Klingenberg, M. Effect of Fatty Acids on H+ Transport Activity of the Reconstituted Uncoupling Protein. *J. Biol. Chem.* **1994**, *269* (4), 2508–2515.

(12)   Al-Awqati, Q. One Hundred Years of Membrane Permeability: Does Overton Still Rule? *Nat. Cell Biol.* **1999**, *1* (8), E201–E202.

(13)   Abel, S.; Galamba, N.; Karakas, E.; Marchi, M.; Thompson, W. H.; Laage, D. On the Structural and Dynamical Properties of DOPC Reverse Micelles. *Langmuir* **2016**, *32* (41), 10610–10620.

(14)   Laage, D.; Elsaesser, T.; Hynes, J. T. Water Dynamics in the Hydration Shells of Biomolecules. *Chem. Rev.* **2017**, acs.chemrev.6b00765.

(15)   Lund, M.; Jönsson, B. Charge Regulation in Biomolecular Solution. *Q. Rev. Biophys.* **2013**, *46* (03), 265–281.

(16)   Egret-charlier, M.; Sanson, A.; Ptak, M. Ionization of Fatty Acids at the Lipid - Water Interface. *FEBS Lett.* **1978**, *89* (2), 313–316.

(17)   Ptak, M.; Egret-Charlier, M.; Sanson, A.; Bouloussa, O. A NMR Study of the Ionization of Fatty Acids, Fatty Amines and N-Acylamino Acids Incorporated in Phosphatidylcholine Vesicles. *Biochim. Biophys. Acta - Biomembr.* **1980**, *600* (2), 387–397.

(18)   Kanicky, J. R.; Poniatowski, A. F.; Mehta, N. R.; Shah, D. O. Cooperativity among Molecules at Interfaces in Relation to Various Technological Processes: Effect of Chain Length on the PKa of Fatty Acid Salt Solutions. *Langmuir* **2000**, *16* (1), 172–177.

(19)   Salentinig, S.; Sagalowicz, L.; Glatter, O. Self-Assembled Structures and PK a Value of Oleic Acid in Systems of Biological Relevance. *Langmuir* **2010**, *26* (14), 11670–11679.

(20)   Pohl, E. E.; Voltchenko, A. M.; Rupprecht, A. Flip-Flop of Hydroxy Fatty Acids across the Membrane as Monitored by Proton-Sensitive Microelectrodes. *Biochim. Biophys. Acta - Biomembr.* **2008**, *1778* (5), 1292–1297.

(21)   Pashkovskaya, A. A.; Vazdar, M.; Zimmermann, L.; Jovanovic, O.; Pohl, P.; Pohl, E. E. Mechanism of Long-Chain Free Fatty Acid Protonation at the Membrane-Water Interface. *Biophys. J.* **2018**, *114*, 2142–2151.

(22)   Morrow, B. H.; Koenig, P. H.; Shen, J. K. Atomistic Simulations of PH-Dependent Self-Assembly of Micelle and Bilayer from Fatty Acids. *J. Chem. Phys.* **2012**, *137* (19), 194902.

(23)   Morrow, B. H.; Eike, D. M.; Murch, B. P.; Koenig, P. H.; Shen, J. K. Predicting Proton Titration in Cationic Micelle and Bilayer Environments. *J. Chem. Phys.* **2014**, *141* (8).

(24)   Bennett, W. F. D.; Chen, A. W.; Donnini, S.; Groenhof, G.; Tieleman, D. P. Constant PH Simulations with the Coarse-Grained MARTINI Model — Application to Oleic Acid Aggregates. *Can. J. Chem.* **2013**, *91* (April), 839–846.

(25)   Vila-Vicosa, D.; Teixeira, V. H.; Baptista, A. M.; Machuqueiro, M. Constant-PH MD Simulations of an Oleic Acid Bilayer. *J. Chem. Theory Comput.* **2015**, *11* (5), 2367–2376.

(26)   Janke, J. J.; Bennett, W. F. D.; Tieleman, D. P. Oleic Acid Phase Behavior from Molecular Dynamics Simulations. *Langmuir* **2014**, *30* (35), 10661–10667.

(27)   Jämbeck, J. P. M.; Lyubartsev, A. P. Derivation and Systematic Validation of a Refined All-Atom Force Field for Phosphatidylcholine Lipids. *J. Phys. Chem. B* **2012**, *116* (10), 3164–3179.

(28)   Jämbeck, J. P. M.; Lyubartsev, A. P. An Extension and Further Validation of an All-

Atomistic Force Field for Biological Membranes. *J. Chem. Theory Comput.* **2012**, *8* (8), 2938–2948.

(29)   Jämbeck, J. P. M.; Lyubartsev, A. P. Another Piece of the Membrane Puzzle: Extending Slipids Further. *J. Chem. Theory Comput.* **2012**, *9* (1), 774–784.

(30)   Jorgensen, W. L.; Chandrasekhar, J.; Madura, J. D.; Impey, R. W.; Klein, M. L. Comparison of Simple Potential Functions for Simulating Liquid Water. *J. Chem. Phys.* **1983**, *79* (2), 926–935.

(31)   Singh, U. C.; Kollman, P. A. An Approach to Computing Electrostatic Charges for Molecules. *J. Comput. Chem.* **1984**, *5* (2), 129–145.

(32)   Bayly, C. I.; Cieplak, P.; Cornell, W.; Kollman, P. A. A Well-Behaved Electrostatic Potential Based Method Using Charge Restraints for Deriving Atomic Charges: The RESP Model. *J. Phys. Chem.* **1993**, *97* (40), 10269–10280.

(33)   Wang, J.; Wang, W.; Kollman, P. A.; Case, D. A. Automatic Atom Type and Bond Type Perception in Molecular Mechanical Calculations. *J. Mol. Graph. Model.* **2006**, *25* (2), 247–260.

(34)   Nosé, S. A Molecular Dynamics Method for Simulations in the Canonical Ensemble. *Mol. Phys.* **1984**, *52* (2), 255–268.

(35)   Parrinello, M.; Rahman, A. Polymorphic Transitions in Single Crystals: A New Molecular Dynamics Method. *J. Appl. Phys.* **1981**, *52* (12), 7182–7190.

(36)   Essmann, U.; Perera, L.; Berkowitz, M. L.; Darden, T.; Lee, H.; Pedersen, L. G. A Smooth Particle Mesh Ewald Method. *J. Chem. Phys.* **1995**, *103* (19), 8577–8593.

(37)   Pokhrel, N.; Maibaum, L. Free Energy Calculations of Membrane Permeation: Challenges Due to Strong Headgroup–Solute Interactions. *J. Chem. Theory Comput.* **2018**, *14* (3), 1762–1771.

(38)   Vermaas, J. V; Beckham, G. T.; Crowley, M. F. Membrane Permeability of Fatty Acyl Compounds Studied via Molecular Simulation. *J. Phys. Chem. B* **2017**, *121* (50), 11311–

11324.

(39)   Hub, J. S.; De Groot, B. L.; Van Der Spoel, D. G-Whams-a Free Weighted Histogram Analysis Implementation Including Robust Error and Autocorrelation Estimates. *J. Chem. Theory Comput.* **2010**, *6* (12), 3713–3720.

(40)   *CRC Handbook of Chemistry and Physics*, 92nd ed.; Haynes, W. M., Lide, D. R., Eds.; CRC Press: Boca Raton, 2011.

(41)   Bonhenry, D.; Tarek, M.; Dehez, F. Effects of Phospholipid Composition on the Transfer of a Small Cationic Peptide across a Model Biological Membrane. *J. Chem. Theory Comput.* **2013**, *9* (12), 5675–5684.

(42)   MacCallum, J. L.; Bennett, W. F. D.; Tieleman, D. P. Distribution of Amino Acids in a Lipid Bilayer from Computer Simulations. *Biophys. J.* **2008**, *94* (9), 3393–3404.

(43)   Abraham, M. J.; Murtola, T.; Schulz, R.; Pall, S.; Smith, J. C.; Hess, B.; Lindah, E. Gromacs: High Performance Molecular Simulations through Multi-Level Parallelism from Laptops to Supercomputers. *SoftwareX* **2015**, *1–2*, 19–25.

(44)   Tribello, G. A.; Bonomi, M.; Branduardi, D.; Camilloni, C.; Bussi, G. PLUMED 2: New Feathers for an Old Bird. *Comput. Phys. Commun.* **2014**, *185* (2), 604–613.

(45)   Frisch, M. J.; Trucks, G. W.; Schlegel, H. B.; Scuseria, G. E.; Robb, M. A.; Cheeseman, J. R.; Scalmani, G.; Barone, V.; Mennucci, B.; Petersson, G. A.; Nakatsuji, H.; Caricato, M.; Li, X.; Hratchian, H. P.; Izmaylov, A. F.; Bloino, J.; Zheng, G.; Sonnenberg, J. L.; Hada, M.; Ehara, M.; Toyota, K.; Fukuda, R.; Hasegawa, J.; Ishida, M.; Nakajima, T.; Honda, Y.; Kitao, O.; Nakai, H.; Vreven, T.; Montgomery Jr., J. A.; Peralta, J. E.; Ogliaro, F.; Bearpark, M. J.; Heyd, J.; Brothers, E. N.; Kudin, K. N.; Staroverov, V. N.; Kobayashi, R.; Normand, J.; Raghavachari, K.; Rendell, A. P.; Burant, J. C.; Iyengar, S. S.; Tomasi, J.; Cossi, M.; Rega, N.; Millam, N. J.; Klene, M.; Knox, J. E.; Cross, J. B.; Bakken, V.; Adamo, C.; Jaramillo, J.; Gomperts, R.; Stratmann, R. E.; Yazyev, O.; Austin, A. J.; Cammi, R.; Pomelli, C.; Ochterski, J. W.; Martin, R. L.; Morokuma, K.; Zakrzewski, V. G.; Voth, G. A.; Salvador, P.; Dannenberg, J. J.; Dapprich, S.; Daniels, A. D.; Farkas, Ö.; Foresman, J. B.; Ortiz, J. V;

Cioslowski, J.; Fox, D. J. Gaussian 09. Gaussian, Inc.: Wallingford, CT, USA 2009.

(46)   Abrams, F. S.; London, E.; Chattopadhyay, A. Determination of the Location of Fluorescent Probes Attached to Fatty Acids Using Parallax Analysis of Fluorescence Quenching: Effect of Carboxyl Ionization State and Environment on Depth. *Biochemistry* **1992**, *31* (23), 5322–5327.

(47)   Kamp, F.; Zakim, D.; Zhang, F.; Noy, N.; Hamilton, J. A. Fatty Acid Flip-Flop in Phospholipid Bilayers Is Extremely Fast. *Biochemistry* **1995**, *34* (37), 11928–11937.

(48)   Kamp, F.; Hamilton, J. A.; Westerhoff, H. V. Movement of Fatty Acids, Fatty Acid Analogues, and Bile Acids across Phospholipid Bilayers. *Biochemistry* **1993**, *32* (41), 11074.

(49)   Gutknecht, J. Proton Conductance Caused by Long-Chain Fatty Acids in Phospholipid Bilayer Membranes. *J. Membr. Biol.* **1988**, *106* (1), 83–93.

(50)   Vorobyov, I.; Olson, T. E.; Kim, J. H.; Koeppe, R. E.; Andersen, O. S.; Allen, T. W. Ion-Induced Defect Permeation of Lipid Membranes. *Biophys. J.* **2014**, *106* (3), 586–597.

(51)   Zhang, H. Y.; Xu, Q.; Wang, Y. K.; Zhao, T. Z.; Hu, D.; Wei, D. Q. Passive Transmembrane Permeation Mechanisms of Monovalent Ions Explored by Molecular Dynamics Simulations. *J. Chem. Theory Comput.* **2016**, *12* (10), 4959–4969.

(52)   Kanicky, J. R.; Shah, D. O. Effect of Premicellar Aggregation on the PKa of Fatty Acid Soap Solutions. *Langmuir* **2003**, *19* (6), 2034–2038.

(53)   Filipe, H. A. L.; Moreno, M. J.; Róg, T.; Vattulainen, I.; Loura, L. M. S. How To Tackle the Issues in Free Energy Simulations of Long Amphiphiles Interacting with Lipid Membranes: Convergence and Local Membrane Deformations. *J. Phys. Chem. B* **2014**, *118* (13), 3572–3581.

(54)   Cevc, G.; Seddon, J. M.; Hartung, R.; Eggert, W. Phosphatidylcholine-Fatty Acid Membranes..Effects of Protonation, Salt Concentration, Temperature and Chain Length on Th e Colloidal and Phase Properties of Mixed Vesicles, Bilayers and Nonlamellar

Structures. *Biochim.Biophys.Acta* **1988**, *940*, 219–240.

(55)   Spector, A. A.; Yorek, M. A. Membrane Lipid Composition and Cellular Function. *J. Lipid Res.* **1985**, *26* (9), 1015–1035.

(56)   Currie, E.; Schulze, A.; Zechner, R.; Walther, T. C.; Farese, R. V. Cellular Fatty Acid Metabolism and Cancer. *Cell Metab.* **2013**, *18* (2), 153–161.

(57)   Hannesschlaeger, C.; Pohl, P. Membrane Permeabilities of Ascorbic Acid and Ascorbate. *Biomolecules*. 2018, p 73.

Table of Contents